CERN - EUROPEAN ORGANIZATION FOR NUCLEAR RESEARCH

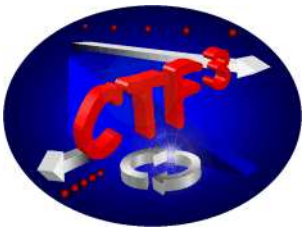

CTF3-Note-092

An Analytical Model for PETS Recirculation

R. Ruber, V. Ziemann
Department of Physics and Astronomy
Uppsala University

Abstract

We derive a simple model that describes the dynamics of the power recirculation scheme for the PETS structures. In particular we describe a method to predict the temporal behavior of the RF power output from the temporal behavior of the electron beam as observed on beam position monitors.

Geneva, Switzerland

March 7, 2009

1 Introduction

The power generation structures (PETS) for CLIC are presently tested [1, 2] in the Two-beam Test Stand (TBTS) that is part of the CTF3 facility at CERN. There the electron beam passes through a PETS structure and both electron beam parameters and the generated RF power are recorded with fast oscilloscopes. Moreover, the PETS structure is equipped with a recirculation mechanism that allows to feed back part of the generated power to the input in order to increase the intra-PETS power level to high levels despite relatively low electron beam currents. A schematic of the setup is shown in Fig. 1. Note that part of the signal is diverted and RF power measurement windows are at the output coupler and the RF-out port, leaving only a fraction of the power to be fed back into the PETS through the input coupler as determined by the variable splitter. Also note the phase shifter which permits to optimize the intra-PETS power by matching the phase of the recirculated fields to the ones generated by the beam, thus allowing to coherently add the effect of different portions of the pulse.

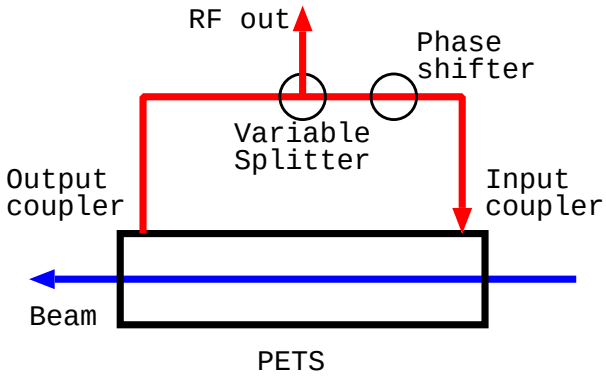

Figure 1: Schematics of the recirculation mechanism. Note that the measurement windows are at the output coupler and at the RF-out port.

In the case without recirculation the temporal profile of the RF-output power is approximately proportional to the square of the beam intensity, because the electric field is proportional to the current and the power flow is proportional to the square of the fields. An example is shown in Fig. 2. Now the question arises whether we can predict the RF-power output from the measured beam intensity in the presence of recirculation. We will address this question in the remainder of the report.

2 Analytical Model

We start by considering the effect of a single bunch, which is approximately equivalent to the impulse response of the system consisting of PETS and the feedback-branch containing the splitter and phase shifter. The effect of a single bunch is easily visualized: it launches a short RF wave-packet into the output coupler. When that packet returns

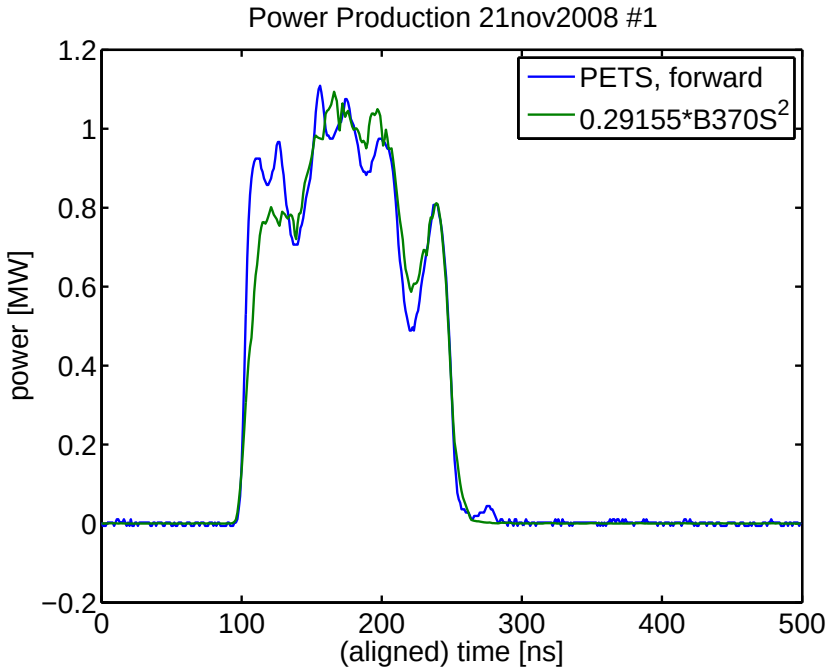

Figure 2: The power and the beam pulse squared.

into the PETS structure after having passed the loop it has undergone an attenuation by a factor $g = e^{-\alpha}$ due to the splitter and losses in the PETS; and a phase shift by an angle ϕ. After two turns the pulse has gone through the loop twice and the field is attenuated twice and has accumulated twice the phase shift. Therefore the impulse response of the intra-cavity PETS power to a single bunch is

$$w(n) = g^n e^{in\phi} = e^{in(\phi+i\alpha)} = q^n \tag{1}$$

where $n = 0, 1, \ldots$ labels the time in units of the loop round-trip time. The different notations are introduced to simplify expressions in the calculations later. Since in practice the recirculated fraction g is considerably less than unity the impulse response is equal to that of a heavily damped harmonic oscillator with a very low $Q-$value. Note that this conceptually resembles the calculation of a wake-potential trailing a point charge.

An important effect of the phase shift is that there are two phases of the RF existent in the PETS, an $I = \mathrm{Re}(w)$ and a $Q = \mathrm{Im}(w)$ channel as can be observed in Fig. 3. The two phases are also visible on the external detector port and this makes the installation of phase-sensitive detectors attractive to be able to diagnose both phases independently.

So far we have only considered the effect of a single bunch but the effect of a train of bunches would be described by the superposition of the effect of many bunches which is mathematically described by a convolution. This is a similar calculation as the transition from the wake-potential of a single particle to the wake-function of an entire bunch. In order to calculate the field at a given time (in units of round-trip time n) we have to sum the field from to all preceding bunches. In the calculation we have to distinguish

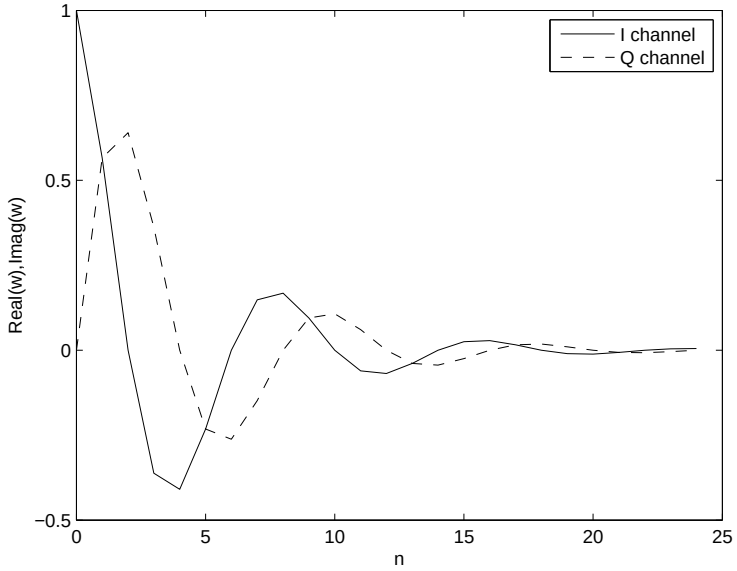

Figure 3: The wake potential $w(n)$ for a recirculation gain $g = 0.8$ and phase shift $\phi = 45$ degree. Observe the large magnitude of the out-of-phase $Q-$channel.

the case where we calculate the field at a time when there are also electron present and the time the bunch has passed. For the sake of simplicity we will assume that we have a rectangular electron pulse $B(k) = B$ with constant beam current for a finite duration $m_1 \leq k \leq m_2$ during which it is driving the PETS. If we have $l < m_1$ we have no field because of causality, but for $m_1 \leq l \leq m_2$ we can calculate the field $f(l)$ by evaluating

$$f(l) = \sum_{k=m_1}^{l} w(l-k)B(k) = B \sum_{k=0}^{l-m_1} e^{ik(\phi+i\alpha)} = B \sum_{k=0}^{l-m_1} q^k \tag{2}$$

where we shifted the summation index $k \to k - m_1$ and used the notation introduced in

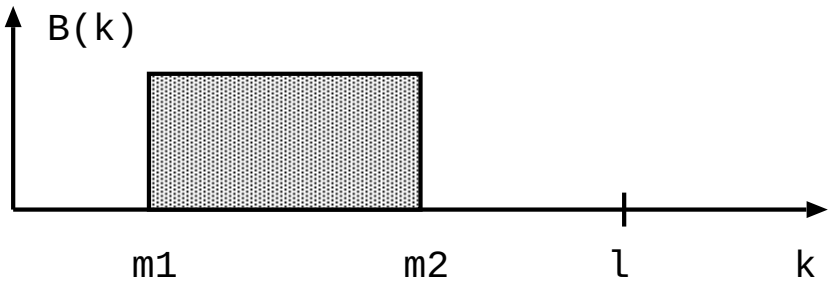

Figure 4: The bunch profile $B(k)$ is constant for $m_1 \leq k \leq m_2$. The field is calculated at a location labeled l.

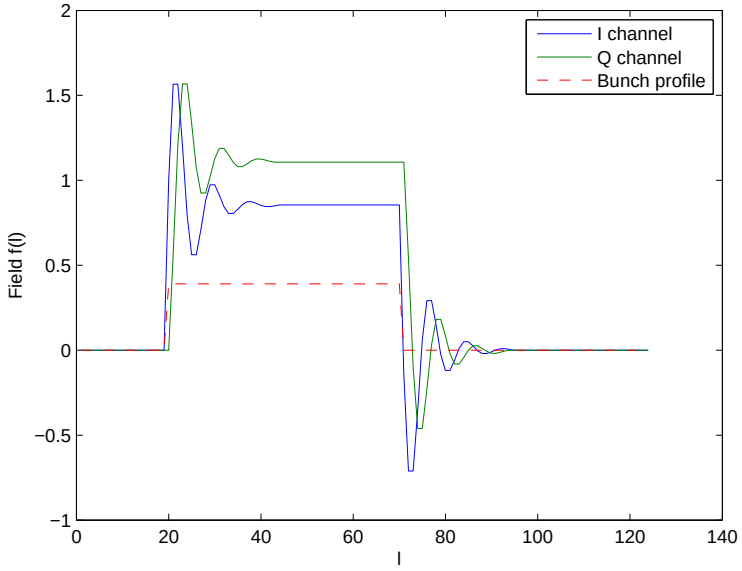

Figure 5: The field in the $I-$ (blue) and $Q-$channel (green) for a bunch (red) that extends from $m_1 = 20$ to $m_2 = 70$ The recirculation parameters are those used in Fig. 3.

Eq. 1. The last expression is just a geometric sum that can be evaluated analytically to be

$$f(l) = B\frac{1-q^{l-m_1+1}}{1-q} \quad \text{for } m_1 \le l \le m_2. \tag{3}$$

For the case that $m_2 < l$ where we need to calculate the field after the bunch has passed and obtain

$$f(l) = B\sum_{k=m_1}^{m_2} w(l-k) = Bq^{l-m_2}\frac{1-q^{m_2-m_1+1}}{1-q} \quad \text{for } m_2 < l \tag{4}$$

and the real and imaginary part of $f(l)$ describe the signals in the I and Q channel, respectively. Note that the field after the bunch as given in Eq. 4, is described by that at the last instance the bunch is present $f(m_2)$ and is recirculating freely, i.e. it accumulates a factor q on every successive turn. We show an example in Fig. 5 for the case already encountered in Fig. 3. Note that in this case the out-of-phase $Q-$channel actually has a higher amplitude than the in-phase $I-$channel. This observation indicates that phase-sensitive diagnostic of the $I-$ and $Q-$channels are indeed desirable. Minimizing the $Q-$channel is actually equivalent to shifting the phase to zero or 180 degree, because in that case the parameter q is real and the field $f(l)$ is also real which means that the imaginary part, the $Q-$channel is zero. This would prove a valuable diagnostic tool.

To this end we note that most of the diagnostic equipment is not sensitive to phases, but only to the intensity, or the power level, which is given by the square of the absolute

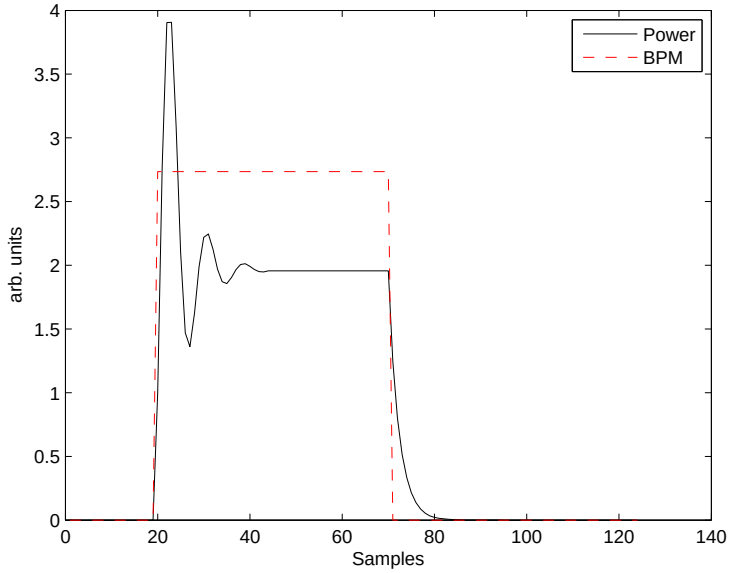

Figure 6: The power (solid) and the bunch profile (dashed). The recirculation parameters are those used in Figs. 3 and 5.

value of the expressions in Eqs. 3 and 4. Even this can be analytically evaluated by introducing the auxiliary complex phase variable $\bar{\phi} = \phi + i\alpha$ with $q = e^{i\bar{\phi}}$ and considering

$$\frac{1-q^N}{1-q} = \frac{e^{-i\bar{\phi}/2}}{e^{-iN\bar{\phi}/2}} \frac{e^{-iN\bar{\phi}/2} - e^{iN\bar{\phi}/2}}{e^{-i\bar{\phi}/2} - e^{i\bar{\phi}/2}} = e^{i(N-1)\bar{\phi}/2} \frac{\sin(N\bar{\phi}/2)}{\sin(\bar{\phi}/2)} \tag{5}$$

and calculating the square of the absolute value

$$\left| \frac{1-q^N}{1-q} \right|^2 = e^{-(N-1)\alpha} \frac{\sin^2(N\phi/2) + \sinh^2(N\alpha/2)}{\sin^2(\phi/2) + \sinh^2(\alpha/2)} \tag{6}$$

where we used the complex trigonometric identity $|\sin(\phi + i\alpha)|^2 = \sin^2\phi + \sinh^2\alpha$. We now utilize this expression to calculate the square of the absolute value of the field $p(l) = |f(l)|^2$ as a function of the position l and arrive at

$$p(l) = B^2 e^{-(l-m_1)\alpha} \frac{\sin^2((l-m_1+1)\phi/2) + \sinh^2((l-m_1+1)\alpha/2)}{\sin^2(\phi/2) + \sinh^2(\alpha/2)} \tag{7}$$

for $m_1 \leq l \leq m_2$ and

$$p(l) = p(m_2) e^{-2(l-m_2)\alpha} \quad \text{for } m_2 < l. \tag{8}$$

The power $p(l)$ for the case corresponding to the figures above is shown in Fig. 6.

We are now in a position to exploit these expression to see how the attenuation g and phase ϕ affect the shape of the RF output pulse for a fixed beam pulse. We use the

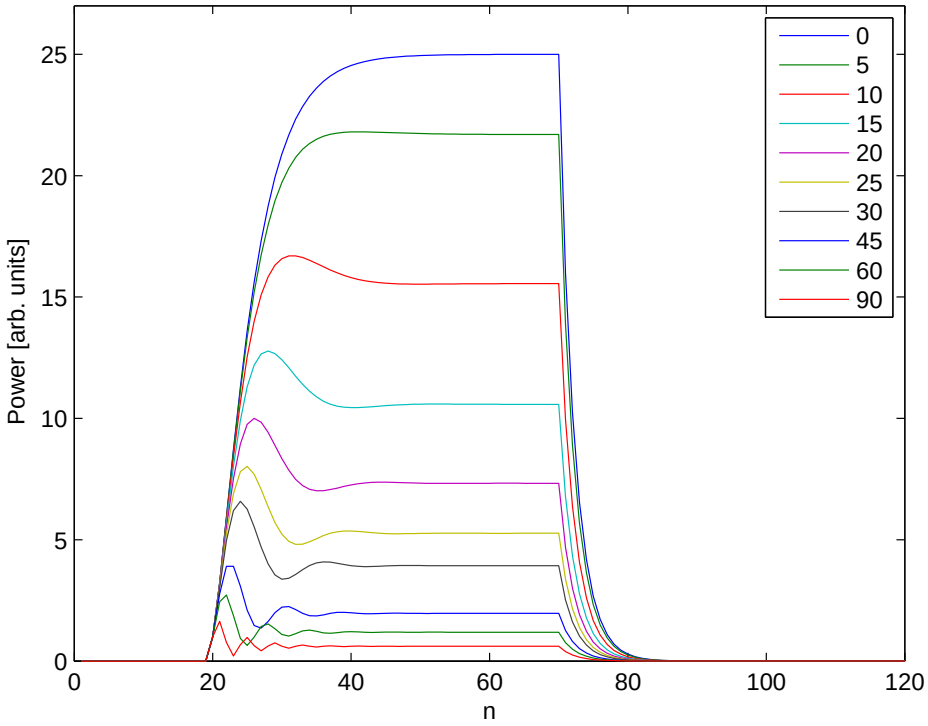

Figure 7: The RF pulse as a function of the phase which varies from zero to 90 degrees.

same beam as before with constant non-zero current from $m_1 = 20$ to $m_2 = 70$, a gain of $g = 0.8$ and vary the phase from zero to 90 degrees. The corresponding pulses are displayed in Fig. 7 where the legend on the right can be used to identify the phase that corresponds to the curves. But it is obvious that the magnitude of the pulse is reduced with increasing phase. We find that a 5 degree phase results in a reduction of about 10 % of the peak power and this figure can be used to define the margin of accuracy required for adjusting the phase. Note also that the pulse form changes qualitatively as the phase is increased: apart from a significantly reduced maximum power level a small peak near the start of the pulse appears. This feature can be used as a qualitative tuning tool to identify a wrongly adjusted phase. Observe that the equations 7 and 8 for the power are symmetric in the phase ϕ and the pulses for negative phases are identical to those of the corresponding positive phase.

This model is restricted in the sense that the sampling time or discretization step is the round-trip time and that the temporal profile of the electron beam is rectangular. These restrictions are cumbersome or impossible to overcome in an analytical model and we therefore discuss a numerical model that will circumvent these drawbacks in the following section.

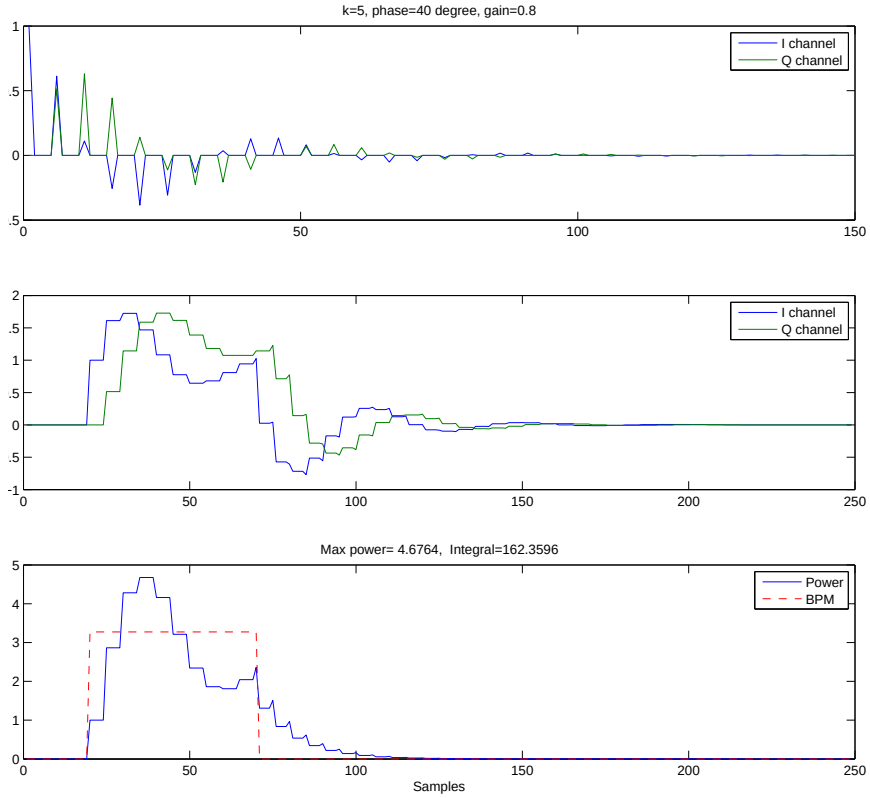

Figure 8: The wake-potential, the fields and the power output for $g = 0.8, \phi = 40$ degree when the ratio of the round-trip time and sampling time is k=5.

3 Numerical Model

The restriction that the round-trip time is longer than the sampling time of beam intensity signal can be easily circumvented by inserting zeros in the wake-potential which means that the wake function is only non-zero at samples that are a multiple of the ratio between round-trip time and sampling time. If we call the ratio k the wake-potential can be written as

$$w(n) = \begin{cases} e^{in(\phi+i\alpha)/k} & \text{if } n = 0, k, 2k, \ldots \\ 0 & \text{else} \end{cases} \tag{9}$$

An example with $k = 5$ is shown in the upper plot of Fig. 8 where we see that there are only non-zero coefficients at multiples of k.

The field $f(l)$ could still be calculated in closed analytical form, but the math becomes rather tedious. It is easier to preform the required convolution in Eq. 2 numerically with the help of Matlab^{TM} [3]. If we assume that the beam intensity signal is stored in an array `bpm` and the real and imaginary part of $w(n)$ from Eq. 9 in arrays `c` and `s`

respectively, the convolution in Matlab can be written as

```
realf = conv(bpm,c);
imagf = conv(bpm,s);
power=realf.^2+imagf.^2;
```

whereby the real and imaginary component of the field f are available in the arrays `realf` and `imagf`, respectively. The power is given by the sum of squares of the real and imaginary field component. Using the same example we used before with a square beam intensity pulse extending from $m_1 = 20$ to $m_2 = 70$ we show the field in the middle graph of Fig. 8 and the power profile (solid) together with the beam intensity profile (dashed) in the bottom graph of Fig. 8. Note that the method used here did not explicitely depend on the shape of the beam intensity signal, such that it would work with any signal.

The code of a function that has as entries the beam intensity signal `bpm`, the phase ϕ, recirculation gain g and the nearest integer of the ratio between bpm sampling time and round-trip time k and returns the `I` and `Q` channel and the power profile `power` is reproduced here.

```
%
% Usage:    [I,Q,power,bpm2]=bpm2power(bpm,phase,gain,k)
%
%  input: bpm   : beam intensity profile
%         phase : recirculation phase in degree
%         gain  : recirculation gain
%         k     : nearest integer of ratio between round-trip time
%                 and bpm sampling time
% output: I     : I-component of the field [arb. units]
%         Q     : Q-component of the field [arb. units]
%         power : power profile, equal to I.^2+Q.^2
%         bpm2  : bpm signal padded with zeros to have the same
%                 length as power
%
function [I,Q,power,bpm2]=bpm2power(bpm,phase,gain,k)
degree=pi/180;
N=30*k;
sp=sin(phase*degree);
cp=cos(phase*degree);
c=zeros(1,N);
s=zeros(1,N);
c(1)=1;        % just one '1' to get impulse response
for j=k+1:N    % recursively build coefficients
    c(j)=gain*(cp*c(j-k)-sp*s(j-k));
    s(j)=gain*(sp*c(j-k)+cp*s(j-k));
```

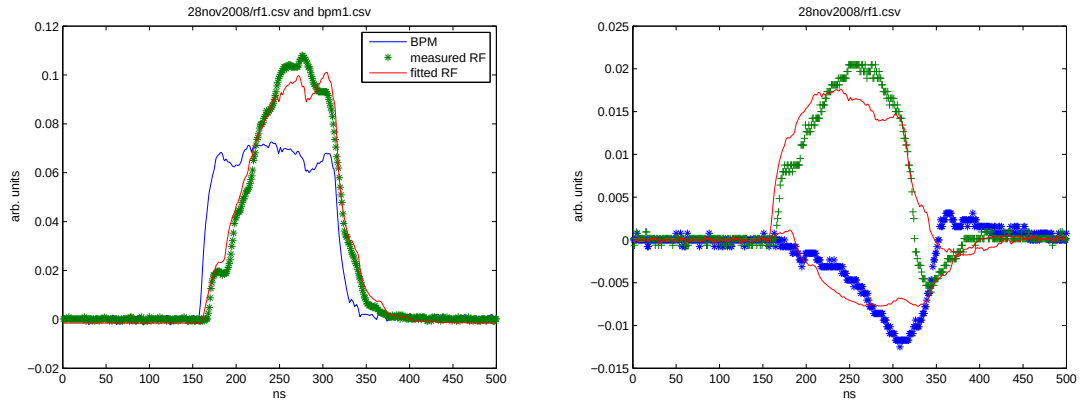

Figure 9: The left plot shows the BPM signal in blue, and the measured and simulated RF power signal in green and red, respectively. The fitted parameters here are $g = 0.52$ and $\phi = 2.8$ degree. On the right hand side the IQ channels and corresponding fits are displayed. We observe that the difference between the measured and fitted parameters is qualitatively satisfactory, especially for the power signal on the left, but there are still differences in the detailed structure, in particular for the IQ-data.

```
end
I=conv(bpm,c);              % I in PETS
Q=conv(bpm,s);              % Q in PETS
power=I.^2+Q.^2;            % power in PETS
bpm2=[bpm zeros(1,N-1)];    % convenient to have in plots
% t=1:length(power); use this as x-axis in plots
return
```

Internally it recursively builds the wake-potential $w(n)$, fills the arrays `c` and `s` and then performs the convolutions with the beam intensity signal `bpm`. In the following section we will use this function to compare measured beam intensity and power signals.

4 Measurements

The presented method can be put to the test by using it in a fit to measured data by minimizing the squared difference of the measured RF data to

```
p(1)+p(2)*bpm2power(bpm_data,p(3),p(4),26)
```

where the four parameters $p(i), i = 1, \ldots, 4$ are the variables that are adjusted. They represent offset, vertical scale, phase, and gain, respectively. Here we also use the fact that the recirculation time is 26 ns. We then set up a cost-function and minimize it with the Matlab function `fminsearch`. Performing the fit to dataset 1 from Nov 28, 2008

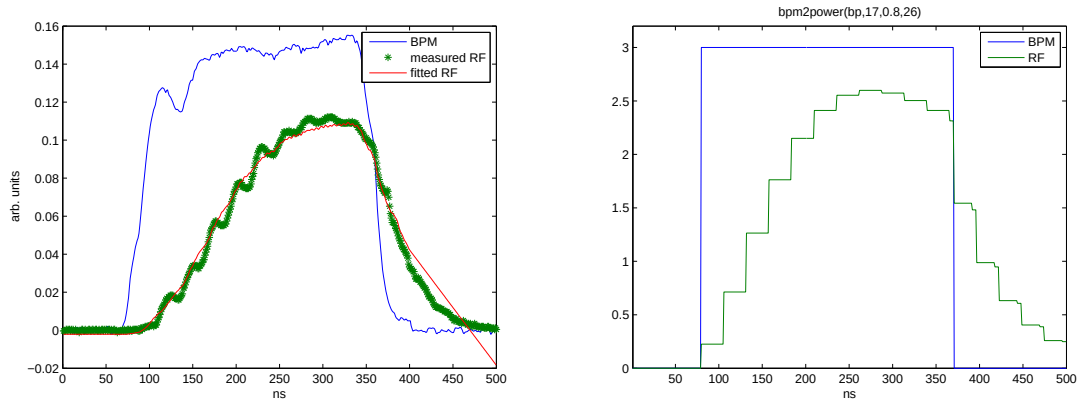

Figure 10: The BPM pulse (blue) and the measured (green) and reconstructed (red) RF power signal are shown on the left. Note that the steps are absent in the reconstructed signal. In an idealized model, shown on the right, where the BPM signal (blue) has infinite bandwidth, the steps in the simulated RF power signal (green) are present. We therefore conclude that the limited bandwidth of the measured BPM data is responsible for the absence of steps in the reconstructed power signal from real data.

we find that the gain is 0.52 and the phase is 2.8 degree. Offset and scale are also determined, but are not relevant here, because they represent electronics offsets and conversion factors. The resulting fit is shown in the left plot of Fig. 9 where we find that the measured (green) and fitted (red) curves agree quite well, especially during the rising and falling edges. There are, however, some differences around the peak, for which we presently cannot offer an explanation.

Since the data files with the RF data also contain measurements of phase sensitive signals from the I and Q channels we attempt to fit these data as well. For this we minimized the difference of the measured I and Q data to cI and cQ that are determined from

```
[I,Q,power]=bpm2power(bpm_data,p(3),p(4),26);
cI=p(2)*(I*cos(p(1))-Q*sin(p(1)));
cQ=p(2)*(I*sin(p(1))+Q*cos(p(1)));
```

where we have introduced the new scale factor $p(2)$ and a phase factor $p(1)$ that accounts for the unknown distance between the PETS structure and the IQ-detector. $p(3)$ and $p(4)$ are the phase and gain as before. Performing the fit yields a phase of about 45 degree and a gain of 0.52, where the former differs significantly from the recirculation phase determined from the power signal. The measured and fitted I and Q signals are shown in the right hand side of Fig. 9 and exhibit a rather poor agreement. Note that we checked that the sum of squares of the I and Q channels agrees well with the measured power signal and can therefore rule out that the discrepancy comes from inconsistent IQ

and power measurements. The poor fit of the IQ data indicates that there are physical mechanisms at work in the PETS that are not accounted for by our simple model with constant gain and recirculation phase.

Some of the data from Dec 11, 2008 exhibit a pronounced staircase behavior as can be seen on the left hand side in Fig 10. When fitting the simulated RF power we find that the overall, global behavior of the curve is well-represented, but that the steps are missing. This puzzling feature is resolved by the observation that the RF signal is sampled at GHz rates and therefore shows the fast temporal behavior, but the BPM data is bandwidth limited at about 200 MHz and therefore smoothes out detailed features in the bunch population. This has the effect of also smoothing out the detailed structure in the simulated RF power derived from the BPM data. As a check we simulated a square pulse and recover the steps as can be seen on the right hand side of Fig. 10. One might consider of trying to de-convolute the response of the BPMs from the recorded BPM data, but this is left for a future note.

5 Conclusions

We derived a simple model for the RF recirculation of the PETS structures presently tested in the Two-Beam Test-Stand. The model was fitted to measured data of power and I-Q signals where the power data agreed quite well but the agreement of simulated to measured IQ data was rather poor indicating that there are effects involved that go beyond the simple model used in this note. One such effect we found stems from the fact that the BPMs are bandwidth limited at a lower frequency than the acquisition system for the RF signals.

We acknowledge discussions and help from Erik Adli with data recording. This work is supported by the Swedish Reserach Council and the Knut and Alice Wallenberg Foundation.

References

[1] I. Syratchev, G. Riddone, S. Tantawi, *CLIC RF High Power production Testing Program,* Proceedings of the European Particle Accelerator Conference EPAC08 in Genoa, June 2008.

[2] I. Syratchev, *PETS and drive beam development for CLIC,* presented at the X-band RF structure and beam dynamics workshop in Daresbury, December 2008.

[3] `http://www.mathworks.com`